Palladium–Magnesium Oxide Nanocatalyst for Selective Hydrogenation: Enhancing Naphtha Stability and Biodiesel Performance

Buthaina Sultan Aziz,[a,*] Jamela Saadi Aziz,[a] Haidar Hasan Mohammed,[b] and Raad Z. Homod[c]

[a]Basra Engineering Technical College, Southern Technical University, Basra, Iraq

[b]Thermodynamics and Mathematical Physics Unit, University of Mons, 7000 Mons, Belgium

[c]Department of Chemical Engineering and Petroleum Refining, Basrah University for Oil and Gas, Basrah, Iraq

doi: https://doi.org/10.15255/CABEQ.2025.2460

Original scientific paper
Received: November 5, 2025
Accepted: March 12, 2026

The hydrogenation of naphtha is critical to producing stable, clean gasoline, yet current catalysts often lack selectivity and stability. In this work, a novel palladium–magnesium oxide (Pd/MgO) nanocatalyst was developed to address these challenges. The catalyst was prepared by reduction of Na_2PdCl_4 on MgO support using sodium borohydride, resulting in well-dispersed Pd nanoparticles with an average size of 1.7 nm and a Pd loading of 0.9 wt.% (nominally 1 wt.%). The size, composition, and dispersion of the nanoparticles were confirmed using transmission electron microscopy, X-ray diffraction, X-ray photoelectron spectroscopy, hydrogen pulse chemisorption, inductively coupled plasma atomic emission spectroscopy, and hydrogen temperature programmed reduction measurements. Catalytic tests showed great activity of quinoline hydrogenation at 150 °C and 40 atm H_2, with a corrected turnover frequency (TOF_{corr}) of 6400 h^{-1}, which was almost fourfold higher than Pd/SiO_2 and Pd/Al_2O_3 commercial catalysts (TOF_{corr} = 1600–1800 h^{-1}). Linear alkenes were hydrogenated with the catalyst at mild conditions (25 °C and 10 atm H_2). Moreover, during biodiesel upgrading, the conversion of polyunsaturated fatty acid methyl esters to stable monounsaturated products was achieved at (100 °C, 1 atm of H_2 with >80 % conversion). Recyclability tests proved that the alkene hydrogenation activity was stable in three cycles, and only slight deactivation in quinoline hydrogenation occurred. This work shows that the Pd/MgO nanocatalysts are promising for enhancing the quality of gasoline, minimizing the formation of gums, and increasing the stability of biodiesel because of their nanoscale dispersion, high selectivity, and recyclability.

Keywords
naphtha hydrogenation, palladium nanocatalyst (Pd NPs), selective hydrogenation

Introduction

Catalytic hydrogenation remains a topic of significant research interest due to its importance in many industrial processes. One of the important reactions that is commonly used in the removal of nitrogen impurities in the feedstock of refinery is referred to as hydrodenitrogenation (HDN). The reaction is applicable since N-heteroaromatic compounds may be partially or completely saturated during HDN[1–5]. N-heterocycles are hydrogenated to store hydrogen and quinoline is hydrogenated to form valuable 1,2,3,4-tetrahydroquinoline intermediate[6]. In turn, alkene hydrogenation plays an important role in conversion of catalytically cracked naphtha to gasoline. The storage durability of biodiesel is significantly improved through selective partial hydrogenation of methyl esters obtained from polyunsaturated fatty acids[7,8], to their monounsaturated equivalents, which increases biodiesel storage stability[9–16].

Despite the wide variety of catalysts available for these reactions, many lack the required activity and selectivity, operate under severe reaction conditions or are prone to deactivation by feed and product impurities. Consequently, there has been a constant demand for new catalysts that do not only have the ability to hydrogenate a broad range of unsaturated substrates under moderate reaction con-

*Corresponding author: botheana.aziz@stu.edu.iq

ditions, but are also not easily poisoned by typical contaminants. Owing to their remarkable selectivity, which are largely related to their small and typically uniform particle size, metal nanoparticles (NPs) constitute an attractive option for developing new catalyst systems[17–19]. In particular, palladium nanoparticles have been used in catalysis in ionic liquids, liquid suspensions, and on solid supports[20–23]. Pd NPs supported on poly (vinylpyrrolidone) have been employed to convert alkynes into alkenes[24] and reduce nitrotoluenes to their respective anilines[25,26]. Similarly, Pd NPs supported on polymers have been used to reduce acetophenone to ethylbenzene through phenylethanol. Cascade reactions involving Heck-type coupling subsequent to carbon-carbon hydrogenation of the resulting transitional product have been observed using Pd/TiO_2[27], Pd/C[28], and with Pd NPs stabilized by ionic liquids, which are either unsupported[29] or dispersed over functionalized multiwalled carbon nanotubes[30]. Palladium nanoparticles supported on hyperbranched aramids have been shown to hydrogenate benzene, phenylacetylene, diphenylacetylene, and quinoline, whereas palladium nanoparticles immobilized on aminomethyl polystyrene bearing hyperbranched dendritic polyamidoamines are capable of reducing five-membered N/O/S heterocycles[31,32]. Palladium nanoparticles supported on silica have been used to hydrogenate phenanthrolines[33], while Pd supported on magnesium oxide has been used as a catalyst to convert phenol primarily to cyclohexanone[34,35].

Previously, it was shown that combining fine metal particles possessing basic properties on the support surface generates NPs capable of facilitating heterolytic H_2 cleavage and ionic hydrogenation of N-heterocycles, as demonstrated for Ru nanoparticles dispersed on poly (4-vinylpyridine) (Ru/PVPy)[36]. While ionic hydrogenation and heterolytic activation of hydrogen are widespread in solution[37], they are rarely observed on solid surfaces. These outer-sphere methods may help prevent catalyst poisoning since neither the feed nor the products need to bind to the reactive metal sites[38,39].

Existing hydrogenation catalysts used for naphtha upgrading and biodiesel stabilization exhibit limited selectivity, are prone to deactivation, and may require harsh operating conditions. Consequently, there remains a critical need for more efficient and sustainable fuel processing. The novelty of this study lies in the development of a palladium-magnesium oxide (Pd/MgO) nanocatalyst containing ultra-small, uniformly dispersed nanoparticles (~1.7 nm) that exhibit high selectivity in the hydrogenation process under mild conditions. It was also intended to design a catalyst with the ability to saturate reactive olefins and diolefins to recover precious aromatics within naphtha, and simultaneously enhance biodiesel stability through controlled partial hydrogenation. Unlike conventional Pd/SiO_2 and Pd/Al_2O_3 catalysts, the strong affinity to metal and basicity of the surface of MgO enhance catalytic activity while suppressing undesirable over-hydrogenation of aromatics. The catalyst offers a flexible platform for naphtha olefin stabilization and biodiesel (FAME) upgrading, contributing to the production of cleaner and more stable fuels.

Materials and methods

Materials

Commercially available Na_2PdCl_4 precursor (Pressure Chemicals, Inc.), as well as reference catalysts (5 % Pd/Al_2O_3, and 5 % Pd/SiO_2) were used in this experiment. Sigma-Aldrich analytical-grade solvents were deoxygenated under nitrogen and purified before use. Substrates and reagents were purified by standard procedures when needed. Magnesium oxide (MgO, 325 mesh, 99 % trace metals basis, Sigma-Aldrich) was pre-calcined in air for two hours at 500 °C before metal loading. Biodiesel was prepared following a conventional protocol. Commercial soybean oil (250 cm^3) was added to a solution of KOH (0.875 g) in methanol (50 cm^3), and the mixture was maintained under stirring for 75 min at 60 °C. After phase separation, the biodiesel layer was heated at 80 °C for 15 min to evaporate the remaining methanol. The product was washed, dried at 110 °C for 20 min, and stored over Na_2SO_4 overnight.

Preparation of Pd/MgO catalyst

For catalyst preparation (1 wt.% Pd/MgO), 2.0 grams of magnesium oxide was placed in a three-neck round-bottom flask that was purged with nitrogen. After adding 10 cm^3 of dry O_2-free methanol, the suspension was stirred. The flask was equipped with two pressure-equalizing dropping funnels, one of which contained Na_2PdCl_4 (0.055 g, 0.02 g Pd) in dry, degassed methanol (10 cm^3), within a few minutes. Na_2PdCl_4 solution was added, followed by $NaBH_4$ at ~1 drop s^{-1}. The resulting dark gray suspension was stirred for 4 h at room temperature under nitrogen. Following filtration under nitrogen, washed three times with methanol (100 cm^3) and left to dry overnight under vacuum at ambient temperature. The same procedure was repeated to prepare 5 wt.% and 10 wt.% palladium on magnesium oxide (Pd/MgO) catalysts using proportionately more Na_2PdCl_4 (0.275 g and 0.55 g, respectively). Metal analysis was performed by ICP-AES on Agilent 5110 spectrometer (Agilent Technologies, USA).

Transmission electron microscopy

TEM analysis was performed using a JEOL TEM-2010 high-resolution microscope. The accelerating voltage of this microscope was 200 kV and the resolution between points was 0.19 nanometers. The samples were prepared by adding a drop of catalyst suspension in hexane to a copper grid and letting it drip dry in the air. Images were recorded using a Gatan OneView digital camera (Gatan, USA), which was attached to TEM.

X-ray diffraction

XRD patterns were recorded using a Philips X'Pert MPD diffractometer with monochromatic Cu Kα radiation (45 kV, 40 mA) in the 2θ range of 20°-90°. Measurements were performed in air at ambient temperature. Prior to analysis, the samples were ground using a mortar.

X-ray photoelectron spectroscopy

XPS measurements were conducted on an Omicron spectrometer fitted with a multichannel hemispherical analyzer and a dual Al/Mg X-ray source using Mg Kα radiation (1253.6 eV). Overall, the sample was placed in powder form on sticky tape. Shirley background had been removed and XPS peaks were then convoluted with curve fitting using XPSPEAKS 4.1. Lorentzian-Gaussian functions (20 % L and 80 % G) were used. The O 1s peak at 529.9 eV of MgO was used as a reference to modify the charging effect[40].

BET surface area analysis

Surface areas of the catalysts, namely the calcined MgO support and Pd/MgO, were assessed using the nitrogen adsorption-desorption technique at 77 K with a Micromeritics ASAP 2020 surface area analyzer (Micromeritics Instrument Corp., USA). The samples were preemptively subjected to vacuum to eliminate physisorbed species.

Hydrogen pulse chemisorption

Chemisorption analysis was conducted using a Micromeritics ChemiSorb 2750 fitted with a TPx controller. After 30 min exposure of the fresh catalyst, following 10 % H_2/Ar treatment at 150 °C, the sample was Ar-purged at 150 °C for another 30 min to eliminate impurities. Once cooled to room temperature, successive pulses of 10 % H_2/Ar were injected until no further H_2 uptake was detected. The gas composition was analyzed using a thermal conductivity detector (TCD). Metal dispersion was calculated using the instrument software assuming 1 atom of H corresponds to 1 atom of Pd[41].

Hydrogen temperature-programmed reduction analysis

H_2-TPR analysis was performed using a Chemisorb 2750 instrument. Approximately 120 mg sample was pretreated in Ar (25 cm^3 min^{-1}) at 200 °C, following cooling to room temperature, the carrier gas was changed to 9.9 % H_2/Ar. A linear heating of the sample to 700 K, at a rate of 10 °C min^{-1}, was initiated after 10 minutes upon TCD baseline stabilization.

Catalytic tests

Hydrogenation of quinolines

The hydrogenation of quinoline, 2-methylquinoline, 3-methylquinoline, and 8-methylquinoline was carried out in a 100 cm^3 glass-lined Parr 5500 reactor equipped with a sampling valve, internal stirrer, thermocouple, and dip tube, and connected to a 4843 controller. Typically, the catalyst, which weighed 100 mg, and the required amount of substrate were mixed with 10 cm^3 of hexane solvent before charging the mixture into the reactor. The mixture was deoxygenated by three separate flushes with H_2 at 20 atm. Subsequently, the reactor was pressurized with hydrogen to 33 atm at ambient temperature, heated to 150 °C under continuous stirring, after which the H_2 pressure increased to 40 atm; the reaction time was set to zero. Reaction progress was monitored by measuring the reacted hydrogen. The end point of the reaction was analyzed by GC–MS, using a Varian 3900 GC coupled to a VF-5ms capillary column and a Saturn 2100T MS. Initial turnover frequencies (TOF_{init}) were estimated from the linear slope of the turnover number (TON) versus t plots. The variation of the individual measurements was not more than 10 percent on average in at least three separate tests that were used to produce the average values of TOF_{corr}.

Hydrogenation of alkenes

Experiments were conducted utilizing a 75 cm^3 5000 Parr multireactor attached to a 4871 controller. The multireactor was also fitted with a thermocouple and a magnetic stirrer. After loading the reactor with the catalyst (100 mg) and 10 cm^3 of C5–C6 olefins (1-pentene and 1-hexene (1:1, v/v)), it was flushed three times with hydrogen at 5 atm, and then pressurized with hydrogen to 10 atm at ambient temperature. Mixing was applied at that moment and a zero reaction time was assigned at the end of the process. Gas analysis was performed using a Shimadzu 2010 GC with an Agilent HP-Al/S capillary column and a flame ionization detector (FID). The experiments were carried out at least in triplicate.

Partial hydrogenation of biodiesel

A 160 cm^3 Parr 5100 low-pressure glass reactor was used to perform the partial hydrogenation of biodiesel. The reactor was also fitted with a stirrer and thermocouple, and interfaced with a 4848 controller. After adding the catalyst (100 mg) and biodiesel (75 cm^3) to the reactor, it was flushed three times with hydrogen at 1 atm. The mixture was brought to the desired temperature under stirring; the event was assigned as a zero reaction time. Under constant H_2 pressure (1 atm), hydrogenation was monitored by periodic sampling at regular intervals of ten minutes. The reaction products were analyzed by GC using the same system as previously described; however, the column and temperature program were adjusted according to the nature of the analyzed products. Conversion and selectivity were determined from GC peak area normalization.

Results and discussion

Catalyst characterization

The 1 wt.% Pd/MgO catalyst that was employed in this study was developed by decreasing Na_2PdCl_4 with an addition of $NaBH_4$ in methanol under ambient temperature. This was done with MgO pre-calcined at 500 °C in the presence of air for 2 h. After the reaction, the initially white solid developed a grayish coloration. After purification, the catalyst was stored in an inert environment. Analogous materials comprising about 5 and 10 wt.% Pd/MgO were obtained by following an identical procedure, with the only variation being the quantity of Na_2PdCl_4 employed. These materials were used primarily for characterization and comparison purposes. ICP-AES analysis revealed actual Pd loading in each of the three catalysts of 0.9 wt.%, 4.4 wt.%, and 9.7 wt.%, respectively. These values were used to determine TOF during catalysis. For simplicity, the samples are referred to throughout this study as Pd/MgO catalysts containing 1, 5, and 10 wt.% Pd.

Transmission electron microscopy

TEM investigation of the fresh 1 wt.% Pd/MgO sample (Fig. 1) showed the existence of Pd particles uniformly distributed on the support surface. The particles had a mean size of 1.7 nm, whereas TEM investigation of fresh samples containing 5 and 10 wt.% Pd/MgO also revealed small palladium nanoparticles, averaging 1.7 and 1.8 nm in diameter, respectively. The 1 wt.% sample was analyzed after it had been used in a run of quinoline hydrogenation at 150 °C and 40 atm H_2, and the result showed that the mean Pd particle size remained largely unchanged; 1.6 nm. These findings suggest minimal catalyst sintering or aggregation, and no significant Pd leaching was observed under the harshest conditions[39].

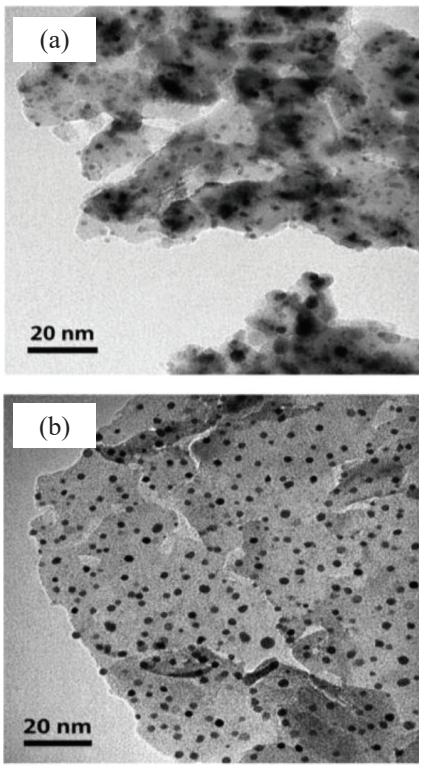

Fig. 1 – *TEM micrographs of 1 wt.% Pd/MgO: (a) fresh catalyst, (b) used catalyst after quinoline hydrogenation at 150 °C and 40 atm H_2*

X-ray photoelectron spectroscopy

The XPS survey spectrum of 1 wt.% Pd/MgO is presented in Fig. 2. Contrary to a comparable catalyst obtained by impregnation, there are no peaks detected ≈200 eV (Cl 2p), indicating a Cl-free catalyst surface that was introduced during the production process[34]. Due to the very low Pd loading, the high-resolution Pd 3d spectrum of 1 wt.% Pd/MgO exhibited very weak signals.

On the other hand, XPS 3d spectra of 10 and 5 wt.% Pd/MgO showed Pd(0) peaks at 335.1 and 339.2 eV (3d5/2, 3d3/2), indicating the existence of metallic palladium on both surfaces[34]; The spectra of both materials showed no other Pd species. It seemed plausible to assume that the surface composition of 1 wt.% Pd/MgO would be comparable, given that all synthesis parameters, except the Pd precursor amount, were the same. In addition, H_2-TPR measurements (which will be discussed further) provide evidence that Pd(0) is either the sole or the predominant species on the surface.

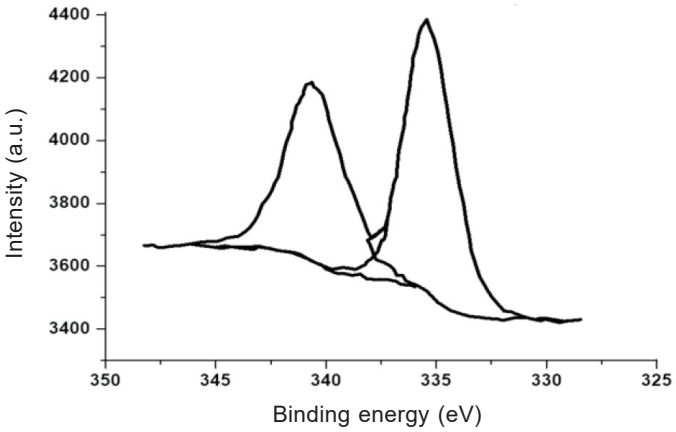

Fig. 2 – *X-ray photoelectron spectroscopy spectrum of the Pd 3d from 10 % Pd/MgO region showing two characteristic peaks*

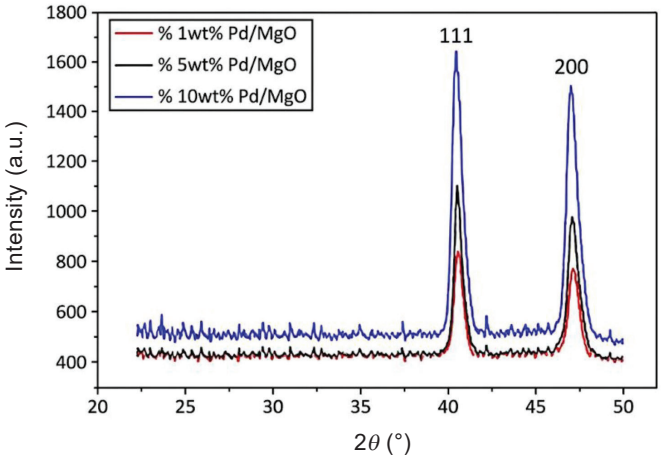

Fig. 3 – *X-ray diffraction patterns of Pd/MgO catalysts showing the characteristic diffraction peaks of metallic Pd at ~40° (111) and 46–47° (200)*

X-ray diffraction

PXRD patterns of the three solids with varying amounts of metal were produced to support the XPS findings on the Pd crystalline phase in the catalyst. As a result of the low metal loading, the Pd diffraction signal of 1 wt.% Pd/MgO material was almost undetectable, similar as in XPS. All 5 peaks were attributed to the MgO phase. For the 5 wt.% Pd/MgO sample, a tiny diffuse peak at $2\theta = 40°$ was observed. This reflection was assigned to Pd(111); nevertheless, the remaining diffraction features of 5 wt.% Pd/MgO could not be distinguished from those of MgO. XRD scans of the 10 wt.% Pd/MgO sample revealed fcc Pd reflections at $2\theta = 40.2°$, 46.8°, and 68.3°, which were attributed to (111), (200), and (220) planes, respectively, matching the standard Pd diffractogram, which are 40.0°, 46.8°, and 68.2°. The dominant MgO (200) reflection at $2\theta = 43.0°$ was used as the internal reference for signal attribution, as shown in Fig. 3.

BET surface area

The physisorption and chemisorption results are provided in Table 1. The specific surface area of the MgO support was 89 $m^2\ g^{-1}$ after calcination at 500 °C for 2 h, and this value was practically maintained following surface deposition of 1 wt.% Pd NPs, i.e., 91 $m^2\ g^{-1}$. The results of hydrogen pulse chemisorption experiments performed on the 1 wt.% Pd/MgO showed that there was about 5 % metal dispersed on the surface. The same 5 wt.% Pd/SiO_2 and 5 wt.% Pd/Al_2O_3 catalysts were tested for comparison of their catalytic performance. This resulted in greater metal dispersion of 11 % and 18 % for the 5 wt.% and 10 wt.% Pd/MgO catalysts, respectively.

The values of the H_2 chemisorption–derived metal dispersion were used in the calculation of the catalytic activities. The dispersion of Pd was estimated by hydrogen pulse chemisorption. To enable a fair comparison between catalysts with different Pd loadings (1 wt.% vs 5 wt.%), catalytic performance was evaluated using dispersion-corrected turnover frequencies (TOF_{corr}) obtained through H_2 chemisorption. Consequently, the discussion focuses on the high catalytic activity observed at low Pd loading, rather than claiming superiority of any specific catalyst. Experiments using H_2-TPR were carried out for 1, 5, and 10 wt.% Pd/MgO, as well as for the MgO support, to assess the reducibility of surface species on Pd/MgO. None among the four samples exhibited positive peaks in their TPR profiles (as shown in Fig. 4), which would indicate hydrogen consumption. The desorption of H_2 that had been adsorbed at room temperature at the beginning of the examination from the surface of metallic Pd results in the negative peaks that are noticed approximately 360 K. Peak intensities paralleled the surface Pd level in each sample. While with the catalyst containing 10 wt.% exhibiting the strongest H_2 desorption peak.

TPR profiles revealed no major reduction processes derived from linear H_2 uptake over the first 1.5–2 h, occurring within a temperature range of 400–700 K. In contrast, the Pd/MgO sample created by impregnation revealed a positive TPR feature at

Table 1 – *Observations from tests of chemical and physical adsorption*

Material	BET surface area ($m^2\ g^{-1}$)	Metal dispersion (%)
MgO	89	N/A
1 % Pd/MgO	91	5 %
5 % Pd/SiO_2	–	11 %
5 % Pd/Al_2O_3	–	18 %

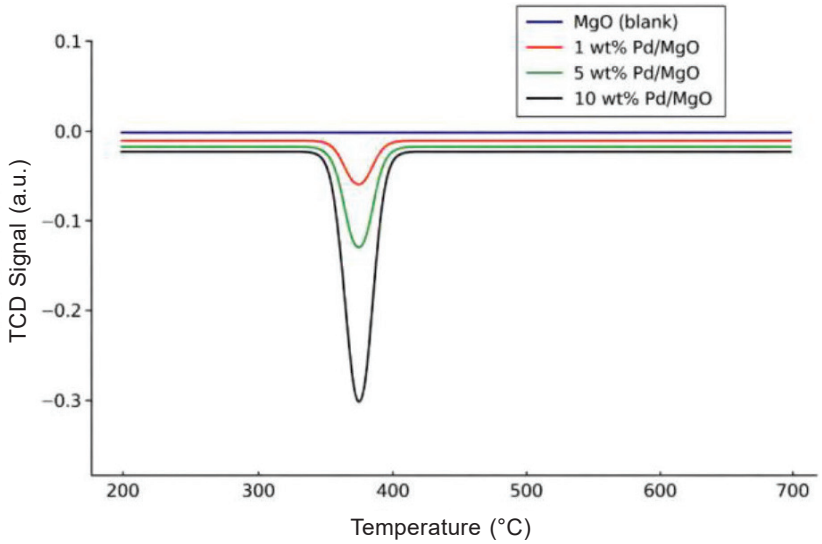

Fig. 4 – *Temperature-programmed reduction (TPR) profiles of MgO and Pd/MgO catalysts with varying Pd loadings*

~450 K linked to PdO, and the three Pd/MgO samples showed TPR behavior corroborated by XRD and XPS. Thus, Pd in these catalysts was predominantly metallic.

Catalytic hydrogenation of quinolines

Hexane or THF may be used as the medium for converting quinoline into 1,2,3,4-tetrahydroquinoline under mild conditions (150 °C, 40 atm); after a few hours, the conversion approaches 100 % with no sign of catalyst deactivation or inhibition caused by the substrate or product. Calculations were derived from linear H_2 uptake over the first 1.5–2 h, giving an initial TOF_{init} = 300 h^{-1}. The value was then dispersion-corrected using H_2 pulse chemisorption (which was estimated to be 5 % in the case of 1 wt.% Pd/MgO). The calculated TOF_{corr} value hit 6400 h^{-1}. This value was used as a measure of catalytic activity. Table 2 summarizes the main hydrogenation results.

As seen in Fig. 5, the values of TOF_{corr} steadily increased with the H_2 pressure within the range of 20–40 atm. This indicates that metal sintering or other forms of catalyst deactivation were negligible at 40 atm H_2 pressure, which aligns with the findings of the TEM study. In the temperature range of 100–150 °C, the catalytic activity similarly increased with temperature. TOF values evaluated across this range were considered adequate, although hydrogenation rates may be boosted even further using greater pressures and temperatures.

The 1 wt.% Pd/MgO catalyst demonstrated high efficiency and selectivity for hydrogenating substituted quinolines under analogous conditions. The presence of a methyl group introduced at the 3-position or 8-position of quinoline slightly decreased the hydrogenation rate, whereas a methyl substituent at the 2-position had no noticeable effect. In all the experiments, hydrogenation was confined to the heterocycle, with no evidence of hydrogenation of the carbocycle.

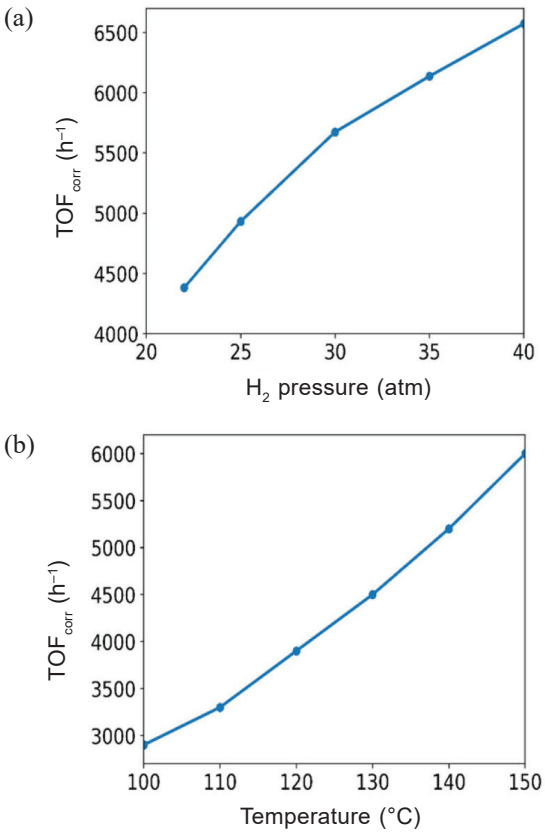

Fig. 5 – *(a) Dependence of corrected turnover frequency (TOF_{corr}) for quinoline hydrogenation using 1 wt.% Pd/MgO on H_2 pressure (20–40 atm); (b) Dependence of TOF_{corr} for quinoline hydrogenation using 1 wt.% Pd/MgO on reaction temperature (100–150 °C)*

Table 2 – *Summary of representative hydrogenation results using 1 wt.% Pd/MgO and commercial reference catalysts*

Reaction system	Catalyst	Temperature (°C)	H_2 pressure (atm)	Main reported outcome
Quinoline hydrogenation	1 wt.% Pd/MgO	150	40	Nearly complete conversion
Quinoline hydrogenation	5 wt.% Pd/SiO_2 (commercial)	150	40	Nearly complete conversion
Quinoline hydrogenation	5 wt.% Pd/Al_2O_3 (commercial)	150	40	Nearly complete conversion
Naphtha relevant olefin hydrogenation	1 wt.% Pd/MgO	25	10	Effective hydrogenation of the tested linear olefins
Biodiesel (FAME) partial hydrogenation	1 wt.% Pd/MgO	100	1	Product mixture enriched predominantly (>80 %) in C18:1 monounsaturated FAMEs

Commercial catalysts with 5 % Pd/SiO_2 and 5 % Pd/Al_2O_3 showed activities that were approximately fourfold below that of our 1 wt.% Pd/MgO catalyst under similar conditions and identical Pd loading. This resulted in TOF_{corr} of 1800 h^{-1}, 1600 h^{-1}, respectively, with respect to quinoline hydrogenation to 1,2,3,4-tetrahydroquinoline. Only one Pd NP catalyst for quinoline hydrogenation on hyperbranched aramids is reported[31]. In the literature scenario, an uncorrected TOF of 350 h^{-1} was reached, on par with ours. There are no studies on substituted quinolines in the literature. Table 2 shows the main hydrogenation results. The Pd/MgO catalyst is highly active at mild conditions, especially in quinoline hydrogenation, and the TOF values are expressed to account for the Pd dispersion. The excellent selectivity that was obtained for the heterocycle saturation may potentially be useful in the production of useful tetrahydroquinoline intermediates.

Catalytic hydrogenation of alkenes

Excess alkenes in naphtha may be reduced by hydrogenation, which is carried out concurrently during the HDS process over regular catalysts. However, if there is an excessive reduction in the amount of olefin present, the fuel's octane rating may see a significant drop as a consequence[7,8]. The octane rating is largely determined by highly substituted, preferential hydrogenation of linear and unsubstituted components primarily. This will result in a higher overall octane rating.

Accordingly, 1 wt.% Pd/MgO was examined for mild hydrogenation of naphtha-representative C5–C6 olefins at 25 °C and 10 atm H_2. Fig. 6 illustrates the olefin hydrogenation conversion profile with time. The catalyst was found to be rapid in the initial activity, and the conversion rate increased steadily at the beginning of the reaction after which it became flat at longer reaction times. This behavior denotes effective hydrogen activation and prolonged catalytic operations in the mild conditions applied (25 °C, 10 atm H_2). Under the same reaction conditions as previous studies, it was shown

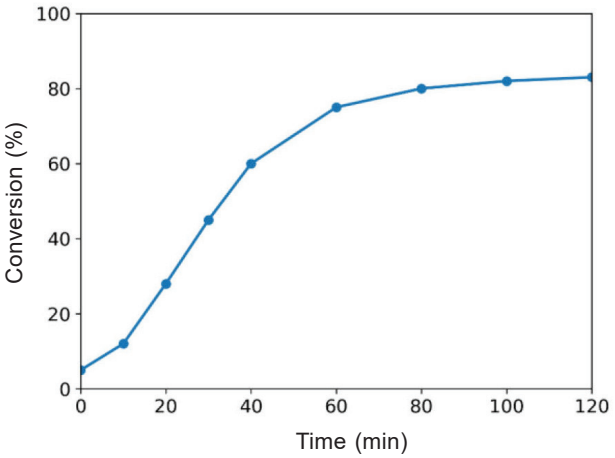

Fig. 6 – *Variation in olefin hydrogenation conversion with reaction time over 1 wt.% Pd/MgO at 25 °C and 10 atm H_2*

that the TOF values for C6-alkene hydrogenation over silica-supported Pd NPs were found to range from 4000 to 38,000 h^{-1} [42,43].

Catalytic hydrogenation of biodiesel

Given the high activity of 1 wt.% Pd/MgO catalyst, its effectiveness was also evaluated in the partial hydrogenation of biodiesel prepared via KOH-catalyzed methanolysis of soybean oil[46]. The catalyst rapidly and selectively converted the FAME mixture to mainly (>80 %) the desired C18:1 at conditions (100 °C, 1 atm H_2), after preliminary screening at optimal conditions (25–100 °C, 1–7 atm H_2). Table 3 presents the biodiesel (FAME) hydrogenation conditions and the obtained results. The data have demonstrated the mild optimized conditions and selective enrichment with C18:1 monounsaturated FAMEs.

Recyclability of the catalysts

Three successive hydrogenations of cyclohexene and quinoline were run with the same 1 wt.% Pd/MgO catalyst to determine the longevity of our catalyst, as well as its capacity to be recycled. The cycle-specific TOF values are shown in Fig. 7,

Table 3 – *Partial hydrogenation of soybean biodiesel (FAME mixture) using a 1 wt.% Pd/MgO catalyst*

Item	Value
Feedstock	Soybean biodiesel (FAME mixture)
Catalyst	1 wt.% Pd/MgO
Screening range	25–100 °C/1–7 atm H_2
Optimized conditions	100 °C/1 atm H_2
Target	Polyunsaturated FAMEs → mono-unsaturated (C18:1)
Main outcome	C18:1 product >80 %

based on normalized hydrogenation activities for each cycle. The hydrogenation activity toward cyclohexene showed approximately a 10 % variation, which is within TOF measurement uncertainty. This indicates that the catalyst remained stable over at least three alkene hydrogenation cycles without experiencing a significant decline of catalytic performance. On the other hand, the activity of quinoline hydrogenation catalyst decreased by around 30 % after the third run. In quinoline hydrogenation recycling, commercial catalysts of 5 % Pd/SiO_2 and 5 % Pd/Al_2O_3 produced results that were comparable to one another in terms of catalytic performance. However, 1 wt.% Pd/MgO showed markedly higher catalytic performance under the same recycling conditions.

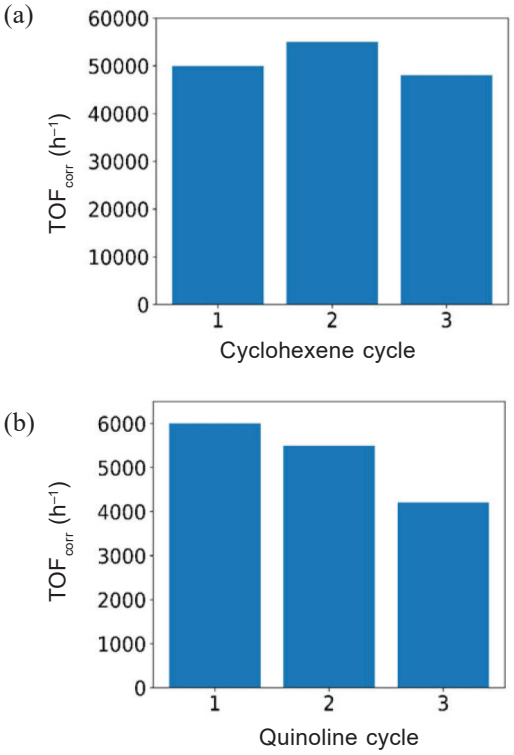

Fig. 7 – *(a) Recyclability of 1 wt.% Pd/MgO in the cyclohexene hydrogenation over three cycles; (b) Recyclability of 1 wt.% Pd/MgO in quinoline hydrogenation over three cycles*

Post-recycling ICP-AES showed negligible Pd loss from the catalyst after quinoline runs (0.9 wt.% used; 0.9 wt.% fresh), with only trace Pd in the organic liquid phase, which may indicate limited but measurable leaching. Consequently, loss in activity was not due to metal leaching. TEM images of the spent catalyst revealed no substantial aggregation of smaller Pd NPs into bigger ones, which would be expected to accompany a decline in catalytic performance. This eliminates the notion that the product 1,2,3,4-tetrahydroquinoline may be inhibiting the reaction. Since a deactivation impact of this kind was not observed during the alkene hydrogenation process, the detected mild drop in activity was probably caused by an unidentified trace impurity in quinoline.

Conclusion

In order to achieve selective hydrogenation under mild conditions, this study proposes a new palladium magnesium oxide (Pd/MgO) nanocatalyst with dispersed Pd nanoparticles (~1.7 nm). The major objective was to develop a useful, stable, and recyclable catalyst to enhance naphtha, quinoline, and biodiesel properties without interfering with fuel quality and over-hydrogenation of aromatics. Some of the key findings of this study include:

- Nanostructure control: TEM analysis was used to control the homogeneous Pd dispersion with an average particle size of 1.7 nm and a high catalytic surface activity.
- Improved quinoline hydrogenation: Under the conditions of 150 °C and 40 atm H_2, the catalyst obtained close to 100 % conversion with a TOF_{corr} of 6400 h^{-1}, which is approximately four times higher compared with commercial Pd/SiO_2 and Pd/Al_2O_3.
- Selective hydrogenation of olefins: The catalyst selectively hydrogenated the linear alkenes at 25 °C and 10 atm H_2.
- Biodiesel upgrading: The monounsaturated FAMEs at 100 °C and 1 atm of H_2 were produced in more than 80 % of the polyunsaturated FAMEs, thereby markedly enhancing oxidative stability.
- Recyclability: Three cycles of alkene hydrogenation were run with stable activity less than 10 % of activity loss; however, quinoline runs experienced a loss of about 30 % which was most likely due to impurities in the substrate.
- Stability: XRD, XPS, and TPR analyses favored the stability of the catalyst in the long run and proved the presence of mainly metallic Pd without PdO formation.

These findings demonstrate that Pd/MgO nanocatalysts provide a stable platform for selective hydrogenation, enhance the stability of gasoline, preserve the quality of fuels, and enhance biodiesel efficiency. The high activity, recyclability, and control at the nanoscale are the characteristics that make them promising for clean fuels.

References

1. *Topsøe, H., Clausen, B. S., Massoth, F. E.,* Hydrotreating Catalysis, in Ertl, G., Knözinger, H., and Weitkamp, J. (Eds.), Catalysis: Science and Technology, Vol. 11, Springer, Berlin, Heidelberg, 1996, pp. 1–269.
2. *Speight, J. G.,* The Desulfurization of Heavy Oils and Residua, 2nd ed., Marcel Dekker, New York, 2000.
3. *Sánchez-Delgado, R. A.,* Organometallic Modeling of the Hydrodesulfurization and Hydrodenitrogenation Reactions, Kluwer Academic Publishers, Dordrecht, 2002.
4. *Kabe, T., Ishihara, A., Qian, W.,* Hydrodesulfurization and Hydrodenitrogenation: Chemistry and Engineering, Wiley-VCH, Kodansha, Tokyo, 1999.
5. *Crabtree, R. H.,* Hydrogen storage in liquid organic heterocycles, Energy Environ. Sci. **1** (2008) 134. doi: https://doi.org/10.1039/B712497D
6. *Murahashi, S. I., Imada, Y., Hirai, Y.,* Rhodium-catalyzed hydrogenation of quinolines and isoquinolines under water–gas shift conditions, Bull. Chem. Soc. Jpn. **62** (1989) 2968. doi: https://doi.org/10.1246/bcsj.62.2968
7. *Brunet, S., Mey, D., Pérot, G., Bouchy, C., Diehl, F.,* On the hydrodesulfurization of FCC gasoline: A review, Appl. Catal. A **278** (2005) 143. doi: https://doi.org/10.1016/j.apcata.2004.10.012
8. *Baricelli, P. J., Lujano, E., Modroño, M., Marrero, A. C., García-Fuentes, Y. M., Sánchez-Delgado, R. A*., Rhodium-catalyzed hydroformylation of C6 alkenes and alkene mixtures: A comparative study in homogeneous and aqueous biphasic media using PPh3, TPPTS and TPPMS ligands, J. Organomet. Chem. **689** (2004) 3782. doi: https://doi.org/10.1016/j.jorganchem.2004.07.035
9. *Di Serio, M., Cozzolino, M., Giordano, M., Tesser, R., Patrono, P., Santacesaria, E.,* From homogeneous to heterogeneous catalysts in biodiesel production, Ind. Eng. Chem. Res. **46** (2007) 6379. doi: https://doi.org/10.1021/ie061648g
10. *Di Serio, M., Tesser, R., Lu, P., Santacesaria, E.,* Heterogeneous catalysts for biodiesel production, Energy Fuels **22** (2008) 207. doi: https://doi.org/10.1021/ef7002504
11. *Falk, O., Meyer-Pittroff, R.,* The effect of fatty acid composition on biodiesel oxidative stability, Eur. J. Lipid Sci. Technol. **106** (2004) 837. doi: https://doi.org/10.1002/ejlt.200400992
12. *Lotero, E., Liu, Y., Lopez, D. E., Suwannakarn, K., Bruce, D. A., Goodwin, J. G.,* Synthesis of biodiesel via acid catalysis, Ind. Eng. Chem. Res. **44** (2005) 5353. doi: https://doi.org/10.1021/ie049157g
13. *Melero, J. A., Iglesias, J., Morales, G.,* Heterogeneous acid catalysts for biodiesel production: Current status and future challenges, Green Chem. **11** (2009) 1285. doi: https://doi.org/10.1039/B902086A
14. *Pinzi, S., Garcia, I. L., Lopez-Gimenez, F. J., Luque de Castro, M. D., Dorado, G., Dorado, M. P.,* The ideal vegetable oil-based biodiesel composition: A review of social, economic and technical implications, Energy Fuels **23** (2009) 2325. doi: https://doi.org/10.1021/ef800988s
15. *Sharma, Y. C., Singh, B., Korstad, J.,* Latest developments in the application of heterogeneous basic catalysts for an efficient and eco-friendly synthesis of biodiesel: A review, Fuel **90** (2011) 1309. doi: https://doi.org/10.1016/j.fuel.2010.10.017
16. *Yang, R., Su, M., Li, M., Zhang, J., Hao, X., Zhang, H.,* One-pot process combining transesterification and selective hydrogenation for biodiesel production from starting material of high degree of unsaturation, Bioresour. Technol. **101** (2010) 5903. doi: https://doi.org/10.1016/j.biortech.2010.02.094
17. *Astruc, D., Lu, F., Aranzaes, J. R.,* Nanoparticles as recyclable catalysts: The frontier between homogeneous and heterogeneous catalysis, Angew. Chem. Int. Ed. **44** (2005) 7852. doi: https://doi.org/10.1002/anie.200500766
18. *Durand, J., Teuma, E., Gómez, M.,* An overview of palladium nanocatalysts: Surface and molecular reactivity, Eur. J. Inorg. Chem. **2008** (2008) 3577. doi: https://doi.org/10.1002/ejic.200800569
19. *Favier, I., Madec, D., Teuma, E., Gómez, M.,* Palladium nanoparticles applied in organic synthesis as catalytic precursors, Curr. Org. Chem. **15** (2011) 3127. doi: https://doi.org/10.2174/138527211797247923
20. *Huang, J., Jiang, T., Gao, H., Han, B., Liu, Z., Wu, W., Chang, Y., Zhao, G.,* Pd nanoparticles immobilized on molecular sieves by ionic liquids: Heterogeneous catalysts for solvent-free hydrogenation, Angew. Chem. Int. Ed. **43** (2004) 1397. doi: https://doi.org/10.1002/anie.200353381
21. *Kormann, H.-P., Schmid, G., Pelzer, K., Philippot, K., Chaudret, B.,* Gas phase catalysis by metal nanoparticles in nanoporous alumina membranes, Z. Anorg. Allg. Chem. **630** (2004) 1913. doi: https://doi.org/10.1002/zaac.200400201
22. *Bronstein, L. M., Chernyshov, D. M., Volkov, I. O., Ezernitskaya, M. G., Valetsky, P. M., Matveeva, V. G., Sulman, E. M.,* Structure and properties of bimetallic colloids formed in polystyrene-block-poly-4-vinylpyridine micelles: Catalytic behavior in selective hydrogenation of dehydrolinalool, J. Catal. **196** (2000) 302. doi: https://doi.org/10.1006/jcat.2000.3039
23. *Tessonnier, J.-P., Pesant, L., Ehret, G., Ledoux, M. J., Pham-Huu, C.,* Pd nanoparticles introduced inside multi-walled carbon nanotubes for selective hydrogenation of cinnamaldehyde into hydrocinnamaldehyde, Appl. Catal. A **288** (2005) 203. doi: https://doi.org/10.1016/j.apcata.2005.04.012
24. *Evangelisti, C., Panziera, N., D'Alessio, A., Bertinetti, L., Botavina, M., Vitulli, G.,* Palladium nanoparticles prepared by sol-immobilization: Synthesis, characterization and catalytic activity in selective hydrogenation reactions, J. Catal. **272** (2010) 246. doi: https://doi.org/10.1016/j.jcat.2010.03.021
25. *Pellegatta, J.-L., Blandy, C., Choukroun, R., Lorber, C., Chaudret, B., Lecante, P., Snoeck, E.,* Palladium colloids from an organometallic route: Redox reaction between [VCp2] and [(Pd(η^3-allyl)Cl)$_2$]. Catalytic application to the hydrogenation of aromatic nitro compounds, New J. Chem. **27** (2003) 1528. doi: https://doi.org/10.1039/B305050B
26. *Drelinkiewicz, A., Waksmundzka, A., Makowski, W., Sobczak, J. W., Król, A., Zieba, A.,* Acetophenone hydrogenation on polymer–palladium catalysts: The effect of polymer matrix, Catal. Lett. **94** (2004) 143. doi: https://doi.org/10.1023/B:CATL.0000029720.69245.6f

27. *Climent, M. J., Corma, A., Iborra, S., Mifsud, M.,* Heterogeneous palladium catalysts for a new one-pot chemical route in the synthesis of fragrances based on the Heck reaction, Adv. Synth. Catal. **349** (2007) 1949. doi: https://doi.org/10.1002/adsc.200700194
28. *Gruber, M., Chouzier, S., Koehler, K., Djakovitch, L.,* Palladium on activated carbon: A valuable heterogeneous catalyst for one-pot multi-step synthesis, Appl. Catal. A **265** (2004) 161. doi: https://doi.org/10.1016/j.apcata.2004.01.020
29. *Jansat, S., Durand, J., Favier, I., Malbosc, F., Pradel, C., Teuma, E., Gómez, M.,* A single catalyst for sequential reactions: Dual homogeneous and heterogeneous behavior of palladium nanoparticles in solution, ChemCatChem. **1** (2009) 244. doi: https://doi.org/10.1002/cctc.200900050
30. *Rodríguez-Pérez, L., Pradel, C., Serp, P., Gómez, M., Teuma, E.,* Supported ionic liquid phase containing palladium nanoparticles on functionalized multiwalled carbon nanotubes: Catalytic materials for sequential Heck coupling/hydrogenation process, ChemCatChem. **3** (2011) 749. doi: https://doi.org/10.1002/cctc.201000383
31. *Tabuani, D., Monticelli, O., Chincarini, A., Bianchini, C., Vizza, F., Moneti, S., Russo, S.,* Palladium nanoparticles supported on hyperbranched aramids: Synthesis, characterization, and some applications in the hydrogenation of unsaturated substrates, Macromolecules **36** (2003) 4294. doi: https://doi.org/10.1021/ma034191n
32. *Guo, Z., Feng, H., Ma, H.-C., Kang, Q.-X., Yang, Z.-W.,* Hydrogenation of five-membered heterocycles of polymer-supported palladium catalyst at normal temperature and pressure, Polym. Adv. Technol. **15** (2004) 100. doi: https://doi.org/10.1002/pat.448
33. *Bianchini, C., Dal Santo, V., Meli, A., Moneti, S., Psaro, R., Sordelli, L., Vizza, F.,* Selective hydrogenation of 1,10-phenanthrolines by silica-supported palladium nanoparticles, Inorg. Chim. Acta **361** (2008) 3677. doi: https://doi.org/10.1016/j.ica.2008.03.021
34. *Claus, P., Berndt, H., Mohr, C., Radnik, J., Shin, E.-J., Keane, M. A.,* Pd/MgO: Catalyst characterization and phenol hydrogenation activity, J. Catal. **192** (2000) 88. doi: https://doi.org/10.1006/jcat.2000.2834
35. *Mahata, N., Raghavan, K. V., Vishwanathan, V., Park, C., Keane, M. A.,* Phenol hydrogenation over palladium supported on magnesia: Relationship between catalyst structure and performance, Phys. Chem. Chem. Phys. **3** (2001) 2712. doi: https://doi.org/10.1039/B102251H
36. *Fang, M., Machalaba, N., Sánchez-Delgado, R. A.,* Hydrogenation of arenes and N-heteroaromatic compounds over ruthenium nanoparticles on poly(4-vinylpyridine): A versatile catalyst operating by a substrate-dependent dual site mechanism, Dalton Trans. **40** (2011) 10621. doi: https://doi.org/10.1039/C1DT11175A
37. *Sandoval, C. A., Ohkuma, T., Muñiz, K., Noyori, R.,* Mechanism of asymmetric hydrogenation of ketones catalyzed by BINAP/1,2-diamine–ruthenium(II) complexes, J. Am. Chem. Soc. **125** (2003) 13490. doi: https://doi.org/10.1021/ja0364989
38. *Rahi, R., Fang, M., Ahmed, A., Sánchez-Delgado, R. A.,* Hydrogenation of quinolines, alkenes, and biodiesel by palladium nanoparticles supported on magnesium oxide, Dalton Trans. **41** (2012) 14490. doi: https://doi.org/10.1039/C2DT31777A
39. *Fang, M., Sánchez-Delgado, R. A.,* Ruthenium nanoparticles supported on magnesium oxide: A versatile and highly selective catalyst for hydrogenation reactions, J. Catal. **311** (2014) 357. doi: https://doi.org/10.1016/j.jcat.2013.12.014
40. *Beckers, N. A., Huynh, S., Zhang, X., Luber, E. J., Buriak, J. M.,* Screening of heterogeneous multimetallic nanoparticle catalysts supported on metal oxides for mono-, poly-, and heteroaromatic hydrogenation activity, ACS Catal. **2** (2012) 1524. doi: https://doi.org/10.1021/cs3002447
41. *Jewell, L. L., Davis, B. H.,* Review of absorption and adsorption in the hydrogen–palladium system, Appl. Catal. A **310** (2006) 1. doi: https://doi.org/10.1016/j.apcata.2006.05.012
42. *Biradar, A. V., Biradar, A. A., Asefa, T.,* Silica-dendrimer core-shell nanospheres with encapsulated ultrasmall palladium nanoparticles: Efficient and easily recyclable heterogeneous nanocatalysts, Langmuir **27** (2011) 14408. doi: https://doi.org/10.1021/la203560d
43. *Domínguez-Quintero, O., Martínez, S., Henríquez, Y., D'Ornelas, L., Krentzien, H., Osuna, J.,* Silica-supported palladium nanoparticles show remarkable hydrogenation catalytic activity, J. Mol. Catal. A: Chem. **197** (2003) 185. doi: https://doi.org/10.1016/S1381-1169(03)00068-5
44. *Bouriazos, A., Sotiriou, S., Vangelis, C., Papadogianakis, G.,* Catalytic conversions in green aqueous media: Part 4. Selective hydrogenation of polyunsaturated methyl esters of vegetable oils for upgrading biodiesel, J. Organomet. Chem. **695** (2010) 327. doi: https://doi.org/10.1016/j.jorganchem.2009.10.021